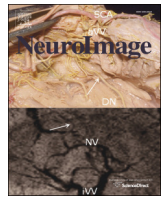




Contents lists available at ScienceDirect

NeuroImage

journal homepage: www.elsevier.com/locate/ynimg

Automated segmentation of multifocal basal ganglia T2*-weighted MRI hypointensities

Andreas Glatz^{a,b}, Mark E. Bastin^{a,b,c,d,*}, Alexander J. Kiker^a, Ian J. Deary^{d,e},
Joanna M. Wardlaw^{a,b,c,d}, Maria C. Valdés Hernández^{a,b,c,d}

^a Brain Research Imaging Centre, Neuroimaging Sciences, University of Edinburgh, Western General Hospital, Crewe Road, Edinburgh EH4 2XU, UK

^b SINAPSE Collaboration, Brain Research Imaging Centre, Neuroimaging Sciences, University of Edinburgh, Western General Hospital, Crewe Road, Edinburgh EH4 2XU, UK

^c Centre for Clinical Brain Sciences, University of Edinburgh, Edinburgh, UK

^d Centre for Cognitive Ageing and Cognitive Epidemiology, University of Edinburgh, Edinburgh EH8 9JZ, UK

^e Department of Psychology, University of Edinburgh, Edinburgh EH8 9JZ, UK

ARTICLE INFO

Article history:

Accepted 3 October 2014

Available online xxx

Keywords:

Magnetic resonance imaging (MRI)

Basal ganglia

Mineralization

Ageing

Focal T2*-weighted MRI hypointensities

Automated segmentation

Outlier detection

ABSTRACT

Multifocal basal ganglia T2*-weighted (T2*w) hypointensities, which are believed to arise mainly from vascular mineralization, were recently proposed as a novel MRI biomarker for small vessel disease and ageing. These T2*w hypointensities are typically segmented semi-automatically, which is time consuming, associated with a high intra-rater variability and low inter-rater agreement. To address these limitations, we developed a fully automated, unsupervised segmentation method for basal ganglia T2*w hypointensities. This method requires conventional, co-registered T2*w and T1-weighted (T1w) volumes, as well as region-of-interest (ROI) masks for the basal ganglia and adjacent internal capsule generated automatically from T1w MRI. The basal ganglia T2*w hypointensities were then segmented with thresholds derived with an adaptive outlier detection method from respective bivariate T2*w/T1w intensity distributions in each ROI. Artefacts were reduced by filtering connected components in the initial masks based on their standardised T2*w intensity variance. The segmentation method was validated using a custom-built phantom containing mineral deposit models, i.e. gel beads doped with 3 different contrast agents in 7 different concentrations, as well as with MRI data from 98 community-dwelling older subjects in their seventies with a wide range of basal ganglia T2*w hypointensities. The method produced basal ganglia T2*w hypointensity masks that were in substantial volumetric and spatial agreement with those generated by an experienced rater (Jaccard index = 0.62 ± 0.40). These promising results suggest that this method may have use in automatic segmentation of basal ganglia T2*w hypointensities in studies of small vessel disease and ageing.

© 2014 The Authors. Published by Elsevier Inc. This is an open access article under the CC BY license (<http://creativecommons.org/licenses/by/4.0/>).

Introduction

Focal hypointensities appear as a frequent feature on T2*-weighted (T2*w) MRI in the basal ganglia of elderly, otherwise healthy, subjects (Glatz et al., 2013). These features are believed to arise from mineralisation in and around penetrating arteries and perivascular spaces (Casanova and Araque, 2003; Morris et al., 1992; Slager and Wagner, 1956), which are possibly of ischemic origin (Janaway et al., 2014). Harder et al. (2008), who studied focal basal ganglia hypointensities on susceptibility-weighted imaging (SWI), found that their degree and hypointensity increase with age, while Penke et al. (2012) demonstrated that their volume correlated negatively with cognitive ability in both youth and older age in a group of 143 community-dwelling subjects in

their seventies. Other studies, such as Aquino et al. (2009) and Li et al. (2014), that have investigated the appearance of the basal ganglia in non-demented elderly subjects on gradient-echo MRI have found that this structure becomes more hypointense with age due to iron storage (Hallgren and Sourander, 1958). However, van Es et al. (2008) reported that increased basal ganglia iron might also be associated with other age-related changes in the brain, such as white matter T2-weighted (T2w) hyperintensities.

MRI has become the de facto standard for assessing iron and mineral deposits in vivo (Haacke et al., 2005; Schenck and Zimmerman, 2004; Valdés Hernández et al., 2012). These trace metal deposits accelerate the realignment of water proton spins in the direction of the main magnetic field and their dephasing in the transverse plane. This causes a localized shortening of T1, T2, and T2* relaxation times and can lead to focal hyperintensities on T1-weighted (T1w) volumes, and focal hypointensities on T2w and T2*w volumes. However, trace metal deposits, such as ferritin, that are separated from water protons by a

* Corresponding author at: Centre for Clinical Brain Sciences, The University of Edinburgh, Western General Hospital, Crewe Road, Edinburgh EH4 2XU, UK.

E-mail address: Mark.Bastin@ed.ac.uk (M.E. Bastin).

water-soluble shell predominantly affect the contrast of T2w and T2*w MRI, whereas they appear isointense on T1w MRI (inner and outer sphere theory; Brass et al., 2006; Schenck, 2003). The T2w and T2*w contrast of trace metal deposits depends on their magnetic susceptibility and their particle radius relative to the average water proton diffusion path length (Weisskoff et al., 1994).

Focal basal ganglia T2*w hypointensities appear predominantly iso- to slightly hypointense on T1w MRI and isointense on T2w MRI which indicates that the underlying mineral deposits are more water-insoluble than ferritin (Vymazal et al., 2000), and consist of aggregated trace metals since this increases reversible dephasing of diffusing water protons (Sedlacik et al., 2014; Weisskoff et al., 1994). Subregions of basal ganglia T2*w hypointensities can also appear very hypointense on T1w MRI which has been linked to advanced mineralization of the underlying tissue, such as calcification (Henkelman et al., 1991; Slager and Wagner, 1956; Valdés Hernández et al., 2014).

Methods for analysing basal ganglia T2*w hypointensities either determine the hypointensity of the whole basal ganglia (Jasinski et al., 2006; Parsey and Krishnan, 1997; van Es et al., 2008) or the volume of focal T2*w hypointensities in individual structures (Valdés Hernández et al., 2011). The former method first classifies all voxels as hypointense that fall below a T2*w threshold which is either derived from the T2*w signal intensities of the red nucleus or globus pallidus. The ratio of hypointense to basal ganglia structure voxels quantifies the degree of hypointensity of each structure. The latest improvements in this method produce reliable results that are in good agreement with those generated by experienced raters (Jasinski et al., 2006). On the other hand, focal T2*w hypointensities in the basal ganglia are still typically segmented semi-automatically (Valdés Hernández et al., 2011). An experienced rater first refines a T2*w threshold equal to the median T2*w signal intensity of the globus pallidus to exclude most artefacts. The rater then manually removes the remaining artefacts based on the visual appearance of focal T2*w hypointensities on T2*w and T1w MRI. An alternative method has also been developed that produces colour maps of the brain with minimum variance quantization of co-registered T2*w and fluid attenuated inversion recovery (FLAIR) volumes (Valdés Hernández et al., 2010). Haemosiderin deposits, which appear green on these maps, are manually identified and included in the final masks. However, validation of these methods shows that both are very time-consuming and associated with high intra-rater variability and low inter-rater agreement (Valdés Hernández et al., 2011).

In this study we therefore developed a fully automated method for segmenting basal ganglia T2*w hypointensities to address the limitations of the previously developed semi-automatic methods. We then investigated the effect of method parameters on the segmentation results in a custom-designed phantom employing several mineral deposit models. The method was also validated with MRI data from a group of community-dwelling subjects in their seventies with a wide range of basal ganglia T2*w hypointensities which have been manually and semi-automatically segmented by two experienced raters. The masks from the manual segmentation were then used to optimise the parameters of the fully automated method, and to assess and compare the accuracy and precision of the masks from the fully automated and semi-automated segmentation.

Methods

Fig. 1 shows an overview of the fully automated method for segmenting basal ganglia T2*w hypointensities. This method generates basal ganglia T2*w hypointensity masks, which possibly indicate basal ganglia mineral deposits (Penke et al., 2012), as well as T2*w/T1w hypointensity masks, which possibly indicate regions of advanced mineralisation, such as calcification (Valdés Hernández et al., 2014). The method generates masks in three steps. Firstly, the structural

T2*w and T1w input volumes are preprocessed, which produces co-registered T2*w and T1w volumes, as well as regions-of-interest (ROI) masks. Secondly, T2*w and T1w thresholds are derived for segmenting focal T2*w hypointensities. Lastly, initial output masks are created by applying these thresholds to the co-registered T2*w and T1w volumes, which are subsequently filtered to reduce thresholding artefacts.

The preprocessing pipeline was mainly implemented in GNU Bash (www.gnu.org) with tools from FSL 5.0 (www.fmrib.ox.ac.uk/fsl) and N4 (www.itk.org), whereas the main processing pipeline was implemented in Matlab 2011b (Natick, MA, USA) with the LIBRA (Verboven and Hubert, 2005) and NIFTI tools (Matlab Central, File ID: #8797). The developed software is available at github.com/aglatz.

Preprocessing pipeline for structural T2*w and T1w MRI

A previously published preprocessing pipeline (Glatz et al., 2013) was used to obtain co-registered T1w and T2*w volumes, as well as caudate, putamen, globus pallidus and adjacent internal capsule masks, which were combined in a ROI mask set. In short, non-brain structures visible on T2*w volumes were automatically removed with FSL BET (Smith, 2002). Non-brain structures visible on T1w volumes were removed by transforming the brain masks created by FSL BET from T2*w to T1w space and by applying them to the corresponding T1w volumes. N4 was used for bias-field correction of all volumes and the T1w volumes were affine registered to the corresponding T2*w volumes using FSL FLIRT (Jenkinson et al., 2002).

To generate the ROI mask set, the basal ganglia nuclei and the thalamus were automatically segmented on the original T1w volumes using FSL FIRST (Patenaude et al., 2011). All structural masks were then linearly transformed from T1w to T2*w space with FSL FLIRT and the previously obtained transformation matrices. Additional internal capsule masks were created by dilating the globus pallidus masks towards the centre of the brain with half disk shaped structural elements of 6 mm radius and then removing regions of these masks that intersected with the union of caudate, putamen, thalamus and globus pallidus masks. The final ROI mask set consisted of four ROI masks, $M_l^{ROI} \subset M$, with the structure labels $l \in \{\text{cn, pu, gp, ic}\}$ corresponding to the caudate nucleus (cn), putamen (pu), globus pallidus (gp) and adjacent internal capsule (ic), where $M \subset \mathbb{Z}^3$ indexes the MRI volume voxel lattice.

Automated threshold selection for segmenting focal T2*w hypointensities

The T2*w intensities of tissue l with focal T2*w hypointensities can be modelled as

$$G_l = (1 - \xi)G_l^{\text{norm}} + \xi G_l^{\text{hypo}}, \quad (1)$$

where the cumulative distribution function of the T2*w intensities G_l are a mixture of normal appearing T2*w tissue intensities and T2*w hypointensities with the cumulative distribution functions G_l^{norm} and G_l^{hypo} , and $0 \leq \xi \leq 1$ as the mixture weight. If both mixture components are normally distributed then methods, such as mixture discriminant analysis (Fraley and Raftery, 2002), can derive an optimal T2*w threshold for dividing the T2*w tissue intensities into normal appearing T2*w tissue intensities and T2*w hypointensities. However, as previously noted (Glatz et al., 2013), T2*w hypointensity distributions typically do not resemble normal distributions, their shapes are variable and their mixture weights are very small ($\xi \ll 1$), hence identifying their underlying parametric distributions is challenging. Therefore T2*w hypointensities were considered outliers of the normal appearing T2*w tissue intensity distribution, which is approximately normally distributed in cases where the signal-to-noise ratio (SNR) is larger than 2 (Gudbjartsson and Patz, 1995).

In this study a previously published robust multivariate outlier detection method (Filzmoser et al., 2005) was adapted for co-registered

Download English Version:

<https://daneshyari.com/en/article/6026685>

Download Persian Version:

<https://daneshyari.com/article/6026685>

[Daneshyari.com](https://daneshyari.com)